

## Imaging of Surface Plasmon Propagation and Edge Interaction Using a Photon Scanning Tunneling Microscope

P. Dawson,<sup>1</sup> F. de Fornel,<sup>2</sup> and J-P. Goudonnet<sup>2</sup>

<sup>1</sup>*Department of Pure and Applied Physics, Queen's University of Belfast, Belfast BT7 1NN, United Kingdom*

<sup>2</sup>*Faculté Sciences Mirande, Laboratoire Physique du Solide, Equipe Optique Submicronique,*

*Université de Bourgogne, BP 138, 21004 Dijon Cedex, France*

(Received 1 November 1993)

We report the direct imaging of surface plasmon propagation on thin silver films using the photon scanning tunneling microscope. It is found that the surface plasmon remains tightly confined in the original launch direction with insignificant scattering to other momentum states. A propagation length of  $13.2 \mu\text{m}$  is measured at  $\lambda = 632.8 \text{ nm}$ . We also present images showing the interaction of a surface plasmon with the edge of the metal film supporting it. The most remarkable feature is the absence of a specularly reflected beam.

PACS numbers: 71.36.+c, 07.60.Pb, 78.66.Bz

The surface plasmon (SP) is a fundamental excitation mode of the interface between a metallic and a dielectric medium. The electromagnetic fields associated with the SP decay exponentially with distance from the interface into each of the bounding media. On the metal side the  $1/e$  field decay length is typically 10–25 nm. If we assume the bounding dielectric medium is air then the field decay length on the air side is of the order of several hundred nm in the visible spectral region—this makes the SP ideal for examination by the photon scanning tunneling microscope (PSTM) [1]. This instrument is the photon analog of the well-known electron STM (eSTM)—a sharpened optical fiber tip probes an evanescent optical field set up at the surface of the sample under scrutiny. In the immediate locality of the tip the evanescent field may couple to propagating modes in the fiber—in effect, photons tunnel across the optical gap between sample and tip. The signal collected by the fiber is utilized in a feedback arrangement to a piezoelectric scanner unit on which the tip is mounted; further details of instrument operation and characteristics are given in Ref. [2]. Very recently the PSTM has been used to probe the SP field above the surface of thin silver films [3,4]. The degree of field enhancement has been monitored [3] and the decay of the SP evanescent field as a function of tip to surface separation has been investigated in detail [4].

A more long-standing theme in the investigation of SPs has been the use of localized launch techniques, in which the width of the stimulating beam is approximately equal to or less than the propagation length of the SP itself. Various studies [5–9] have exploited localized launching to obtain fundamental information on SP excitation and decay; a brief critique of those experiments is given later. In the present study the use of the PSTM is combined with localized launching of SPs to yield detailed *images* of SP propagation for the first time. In the first part of this Letter we present a description of the experiment and of results illustrating the launch and propagation of SPs on a thin silver film. In the second part images are

presented which show the interaction of a SP with the edge of a silver film.

In our experiment SPs are excited in a prism coupling or attenuated total reflection (ATR) arrangement [10]. Wave vector matching to the mode at the silver-air interface in a prism-silver-air system is achieved when light is internally incident on the silver film at an angle just above the prism critical angle. The optical input configuration to the prism, which is mounted in the PSTM head, is illustrated in Fig. 1. It consists of two input beams which each excite SPs at the silver-air interface. An unfocused control beam from a green HeNe laser ( $\lambda_1 = 543.5 \text{ nm}$ ) is used for feedback control of the tunneling tip. The second beam, from a red HeNe laser ( $\lambda_2 = 632.8 \text{ nm}$ ), is focused to a spot within the area of the control beam thus giving localized launching of “red”

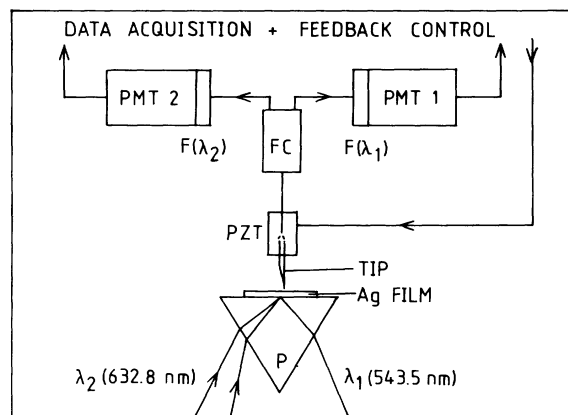


FIG. 1. Optical input scheme for the PSTM with simultaneous excitation of surface plasmons on the Ag-air interface at two different wavelengths: unfocused control beam, of wavelength  $\lambda_1$ , for feedback control of tunneling tip and focused probe beam, of wavelength  $\lambda_2$ , for localized launching of surface plasmons. Various components are P: prism; PZT: piezoelectric scanner tube; FC:  $2 \times 2$  fiber coupler; F: optical interference filter; PMT: photomultiplier tube.

SPs. Separate detection of the signals at the two wavelengths is achieved using a  $2 \times 2$  fiber coupler in conjunction with optical bandpass filters of appropriate center wavelengths (see Fig. 1). When an area of the sample is scanned two images are simultaneously recorded at the two wavelengths. The PSTM was used in the constant current mode of operation in which the tip scans contours of constant evanescent field intensity. The control beam image thus maps tip movement in the  $z$  direction as a function of position in the  $x$ - $y$  or sample plane, while the probe beam image maps the corresponding red signal intensity at each point in the scan. The results which we will present were taken on two silver films (53 and 58 nm thick) produced by thermal evaporation onto clean,  $60^\circ$  silica prisms at a pressure of  $5 \times 10^{-5}$  Pa. The fiber tips were produced by etching in hydrofluoric acid the end of one of the fiber inputs to the coupler.

The image of Fig. 2 (a) shows the evanescent field intensity of a focused red beam on a bare (uncoated) section of the prism. It consists of a peak of Gaussian section with a long axis of  $12.4 \mu\text{m}$  in the  $x$  direction and a short axis of  $7.9 \mu\text{m}$  in the  $y$  direction; the axes lengths are determined from the  $1/e$  [2] intensity points. When the spot is moved onto the silver film at the SP resonance angle it acquires a very pronounced, exponentially decaying tail on one side only vividly demonstrating SP propagation—see Fig. 2(b). Clearly the propagation of the SP leads to the detection of a signal outside the driven field region. The  $1/e$  propagation length of the SP,  $L_{SP}$ , is determined to be  $13.2 \mu\text{m}$  from line scans of the exponentially decaying tail section. A further important observation is the good lateral confinement of the SP [see inset of Fig. 2(b)]. Full 3D imaging of SP propagation allows us to make a direct, quantitative measurement of the effects of elastic SP-SP scattering. Taking line sections in the  $y$  direction it is found that the width of the SP beam increases monotonically from  $9.2 \mu\text{m}$  at the launch site (slightly greater than the spot width on the bare silica) at a rate of  $0.45 \mu\text{m}$  per  $10 \mu\text{m}$  traveled in the  $x$  direction. Of this spread we estimate  $\sim 0.09 \mu\text{m}$  to be due to the angular spread at launch. In the case of both images presented in Figs. 2(a) and 2(b) the corresponding green, control beam images are flat and featureless.

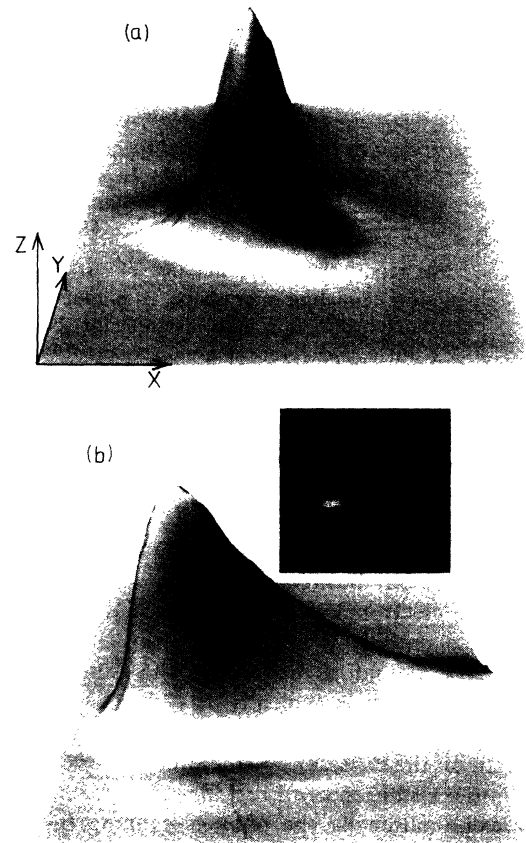


FIG. 2. (a) PSTM image of evanescent field intensity of focused red ( $\lambda = 632.8 \text{ nm}$ ) beam internally incident on bare (uncoated) prism face at greater than critical angle, as in scheme of Fig. 1. Scan range is  $40 \mu\text{m} \times 40 \mu\text{m}$ . (b) PSTM image of the same red beam spot as in (a), but with beam directed onto 53 nm thick silver film, exciting surface plasmon. The exponentially decaying tail is due to surface plasmon propagation. Scan range is  $40 \mu\text{m} \times 40 \mu\text{m}$ . Inset: two-dimensional version of image.

Let us consider in more detail the measured value of  $L_{SP}$  in the context of the basic theory of SPs on systems with planar interfaces. The implicit dispersion/damping relation for SPs in a three-media, two-interface system may be expressed as [11]

$$\left( \frac{\epsilon_1}{k_1} + \frac{\epsilon_2}{k_2} \right) \left( \frac{\epsilon_2}{k_2} + \frac{\epsilon_3}{k_3} \right) + \left( \frac{\epsilon_1}{k_1} - \frac{\epsilon_2}{k_2} \right) \left( \frac{\epsilon_2}{k_2} - \frac{\epsilon_3}{k_3} \right) e^{-2k_2 d_2} = 0, \quad k_n = \left( k_x^2 - \frac{\omega^2}{c^2} \epsilon_n \right)^{1/2} \quad (1)$$

The various  $k_n$  are the field decay constants normal to the interfaces and the values  $n=1,2,3$  may be taken to denote the prism, silver film, and air, respectively; the  $\epsilon_n$  denote the optical dielectric response functions. The propagation vector is  $k_x$ ; the imaginary part,  $k_{xi}$ , describes the damping which may be expressed in terms of the propagation length,  $L_{SP} = 1/2k_{xi}$ . Equation (1) is established through the use of Maxwell's equations and the

application of appropriate boundary conditions. However, the problem is structured in such a way that there is no stimulating field term and this is a significant point. It means that Eq. (1) applies only to *freely* propagating excitations outside a stimulating field region. It should thus be applicable only to the exponential tail region of the SP propagation images acquired in this investigation. Solv-

ing for  $k_x$  numerically with  $\epsilon_{\text{prism}}=2.123$  and  $\epsilon_{\text{Ag}}=-17.9+i0.7$  (Ref. [12]) the value of  $L_{\text{SP}}$  in the thick film limit ( $t_{\text{Ag}} \geq 120$  nm) is found to be  $42.4 \mu\text{m}$ . This length is considerably greater than the experimental value of  $13.2 \mu\text{m}$ . However, if the calculation is performed for the case of the film thickness pertinent to the results presented here ( $t_{\text{Ag}}=53$  nm) it is found that  $L_{\text{SP}}=24.3 \mu\text{m}$ , somewhat closer to the measured value. Physically, the reason for the dramatic reduction in  $L_{\text{SP}}$  with the decreased film thickness is the coupling of the excitation to bulk EM modes in the prism. Thus, beyond the launch site the freely propagating SP has open to it both an intrinsic damping channel (which give rises to a value of  $42.4 \mu\text{m}$  for  $L_{\text{SP}}$ ) and a significant radiative decay channel into the prism. The radiative decay channel is necessarily present since the inverse photon-SP coupling process is used to launch the SP; its magnitude is clearly film thickness dependent. There is no significant reduction in the measured value of  $L_{\text{SP}}$  due to scattering to other SP momentum states of equal magnitude. A more accurate, calculated value would be achieved by taking into account an overlayer of silver sulphide, off-resonance launching of the SP (the converging input beam fills the SP reflectance dip), and an experimentally determined value of  $\epsilon_{\text{Ag}}$  for the film concerned.

In earlier work [5,6] on localized launching of SPs a single, unfocused laser beam was used to excite modes for which  $L_{\text{SP}}$  was comparable to or larger than the beam diameter. This involved working in the infrared spectral region [5] or in geometries in which long range coupled SP modes are supported [6]. Propagation of the SP was monitored by comparing the spatial profile of the reflected beam with that of the input beam; the former was influenced in a nonlocal fashion by the reradiation of the SP into the prism outside the launch site. The constriction of having a large value of  $L_{\text{SP}}$  was overcome in sophisticated, time-resolved pump and probe beam experiments [7,8], in which both beams were focused to spots of diameter  $< 10 \mu\text{m}$ . Propagation of SPs was measured *indirectly* by detecting small changes in the probe beam reflectance due to variations in  $\epsilon_{\text{Ag}}$  induced by the decay of the pump beam stimulated SP. The technique yields fundamental information on electron and lattice heating but is not well adapted to imaging—that would involve rastering the probe beam and measuring a reflectance change of the order of  $10^{-4}$  to  $10^{-5}$  for each point, with resolution determined by a convolution of the (diffraction limited) pump and probe SP spatial intensity profiles. Finally we note that Kroo *et al.* [9] first reported the use of eSTM to measure the propagation of locally launched SPs; line scans only are presented. Detection is through SP related changes in the tunnel current which are due either to thermal expansion (primarily of the Ag film) or by rectification of the SP ac field in surface regions of highly nonlinear  $I$ - $V$  characteristics. By comparison with the experiments discussed above, the particular strengths of the PSTM technique are the *direct* probing of the SP

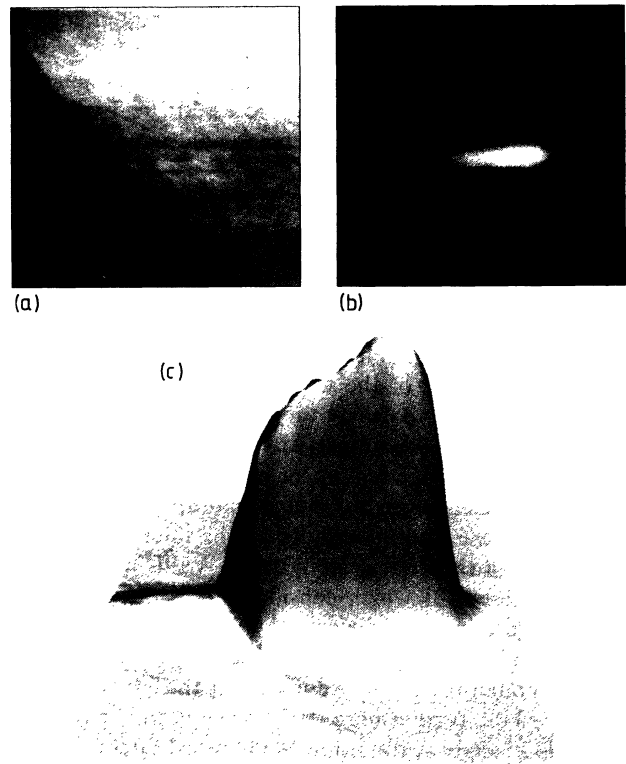


FIG. 3. PSTM images of  $40 \mu\text{m} \times 40 \mu\text{m}$  scan taken across edge of 58 nm thick silver film in arrangement of Fig. 1. (a) Two-dimensional green ( $\lambda=543.5$  nm) control beam image showing silver edge; the silver film lies to upper-right side of image and silica surface to lower-left side. Optical height of edge is 575 nm. (b) Corresponding, two-dimensional red ( $\lambda=632.8$  nm) probe beam image showing surface plasmon incident on edge of silver film from right hand side. (c) Three-dimensional version of (b) showing abrupt truncation of surface plasmon at silver edge.

evanescent field and the consequent capability of *imaging* SPs. In addition the subwavelength resolution, determined by the tip dimension, is better than that of the other all-optical techniques and the PSTM scores over eSTM in that it can operate over dielectric regions. These advantages are now exploited in observing the interaction of a SP with the edge of a silver film, where the film meets the silica substrate.

Figure 3(a) shows the 2D control beam ( $\lambda=543.5$  nm) image with the silver film lying to the top, right hand side and the silica substrate to the lower, left hand side. This image was obtained by impinging the unfocused control beam on an area covering the edge region at an angle of incidence such that the SP was excited on the silver film; the direction of SP propagation was *away* from the edge. The edge, defined by masking during deposition of the silver film, is not abrupt, extending  $\sim 3.5 \mu\text{m}$  between the silica substrate and the full-thickness silver region. This measurement was subsequently confirmed in atomic force microscope images of the same edge region; a film thick-

ness of 58.1 nm was also determined. In the optical picture the edge appears 575 nm high; however, this is an optical height, determined essentially by the efficiency of coupling to the SP and the degree of SP field enhancement [3] relative to the evanescent field extending over the bare substrate region.

The images of Figs. 3(b) and 3(c) show a red SP propagating from right to left *towards* the edge of the silver film. Examining the 2D image [Fig. 3(b)] the most striking feature is the lack of any specularly reflected SP beam. No evidence of any such beam was found in numerous edge scan images. The abrupt truncation of the SP at the edge of the film is clearly seen in the 3D image of Fig. 3(c). Clearly the SP energy is either radiated or absorbed; we suggest that the SP driven charge oscillation at the edge region constitutes an efficient, radiating mechanism, even for the nonabrupt edges studied here. These are the first results on the microscopic scale pertinent to a theoretical analysis by Wallis, Maradudin, and Stegeman [13] which considered SPs incident on an abrupt edge in various dielectric environments. Selecting from that analysis the geometry which corresponds most closely to our experiment we note that the SP reflectance is only  $\sim 0.02$ ; furthermore the "transmitted" or radiated energy is strongly scattered in the forward direction. Absorbed energy cannot be measured in our experiment but a radiatively scattered component may be detected. Scanning at greater tip to sample separation the photon image becomes less intense at all points but in an uneven fashion, with a peak developing at the silver edge and a relative strengthening of the tail extending over the silica surface. These features are due to the collection of scattered radiation which has a much weaker  $z$  dependence than the exponential decay of the SP fields [2]. Again there is a qualitative correlation between the highly directional tail over the silica surface and the strong forward scattering described in Ref. [13]. Pickup of the scattered light by the fiber tip may account for the uneven nature and more linear decay of the SP intensity profile in Fig. 3(c).

In summary, we have constructed a focused probe

beam/unfocused control beam input arrangement to the PSTM which facilitates the direct imaging of SP launch from a localized site and of subsequent propagation. In addition to giving a direct measurement of  $L_{SP}$ , the images yield novel, microscopic scale information on elastic SP-SP scattering and on SP interaction with a silver film edge. We consider the technique has the potential to break open the physical optics of SPs and other surface polariton type excitations in general.

P.D. would like to acknowledge the CNRS, France and the Royal Society, United Kingdom for funding a study visit to the Universite de Bourgogne, Dijon, during which this work was performed. We are most grateful to Y. Lacroute and C. Aquilina for technical support and K. W. Smith for assistance with the production of the images. Laboratoire Physique du Solide, Equipe Optique Submicronique is associée au CNRS.

- 
- [1] R. C. Reddick, R. J. Warmack, and T. L. Ferrell, *Phys. Rev. B* **39**, 767 (1989).
  - [2] R. C. Reddick *et al.*, *Rev. Sci. Instrum.* **61**, 3669 (1990).
  - [3] O. Marti *et al.*, *Opt. Commun.* **96**, 225 (1993).
  - [4] P. M. Adam *et al.*, *Phys. Rev. B* **48**, 2680 (1993).
  - [5] W. P. Chen, G. Ritchie, and E. Burstein, *Phys. Rev. Lett.* **37**, 993 (1976).
  - [6] H. Dohi, S. Tago, M. Fukui, and O. Tada, *Solid State Commun.* **55**, 1023 (1985).
  - [7] M. van Exter and A. Lagendijk, *Phys. Rev. Lett.* **60**, 49 (1988).
  - [8] R. H. M. Groeneveld, R. Sprik, and A. Lagendijk, *Phys. Rev. Lett.* **64**, 784 (1990).
  - [9] N. Kroo *et al.*, *Europhys. Lett.* **15**, 289 (1991).
  - [10] E. Kretschmann and H. Raether, *Z. Naturforsch. A* **23**, 2135 (1968).
  - [11] C. A. Ward *et al.*, *J. Chem. Phys.* **62**, 1674 (1975).
  - [12] P. B. Johnston and R. W. Christie, *Phys. Rev. B* **6**, 4370 (1972).
  - [13] R. F. Wallis, A. A. Maradudin, and G. I. Stegeman, *Appl. Phys. Lett.* **42**, 764 (1983).

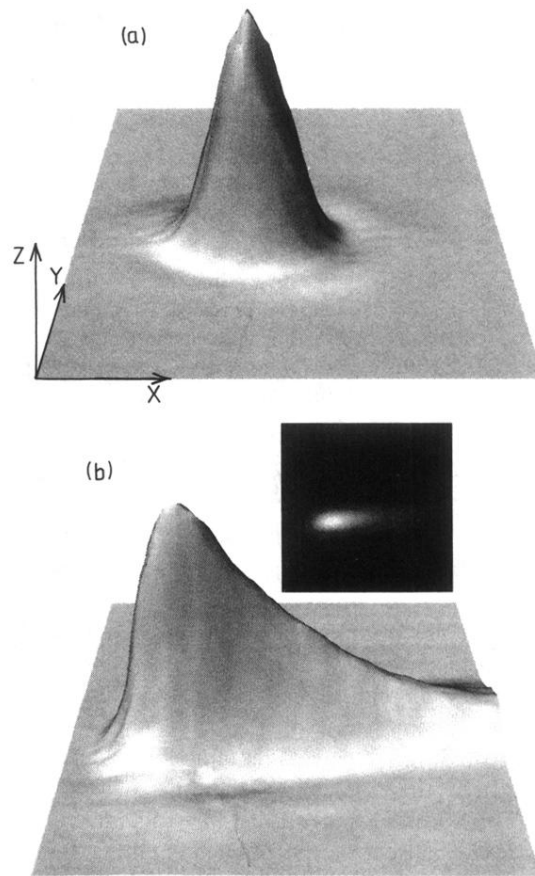


FIG. 2. (a) PSTM image of evanescent field intensity of focused red ( $\lambda = 632.8$  nm) beam internally incident on bare (uncoated) prism face at greater than critical angle, as in scheme of Fig. 1. Scan range is  $40 \mu\text{m} \times 40 \mu\text{m}$ . (b) PSTM image of the same red beam spot as in (a), but with beam directed onto 53 nm thick silver film, exciting surface plasmon. The exponentially decaying tail is due to surface plasmon propagation. Scan range is  $40 \mu\text{m} \times 40 \mu\text{m}$ . Inset: two-dimensional version of image.

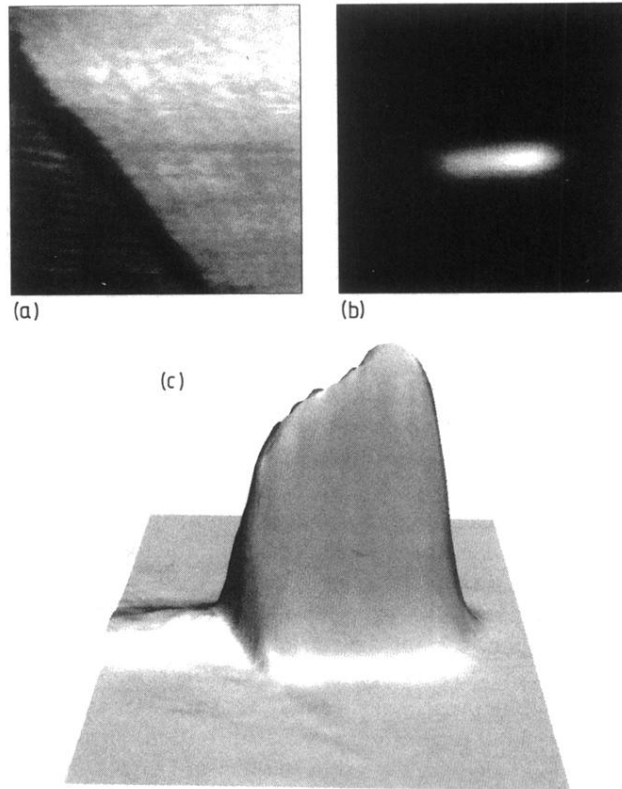


FIG. 3. PSTM images of  $40\ \mu\text{m} \times 40\ \mu\text{m}$  scan taken across edge of 58 nm thick silver film in arrangement of Fig. 1. (a) Two-dimensional green ( $\lambda = 543.5\ \text{nm}$ ) control beam image showing silver edge; the silver film lies to upper-right side of image and silica surface to lower-left side. Optical height of edge is 575 nm. (b) Corresponding, two-dimensional red ( $\lambda = 632.8\ \text{nm}$ ) probe beam image showing surface plasmon incident on edge of silver film from right hand side. (c) Three-dimensional version of (b) showing abrupt truncation of surface plasmon at silver edge.